

Crystal and molecular structure determination, TGA-DTA, and infrared and Raman spectra of rubidium nitroprusside, $\text{Rb}_2[\text{Fe}(\text{CN})_5\text{NO}]$

D. B. Soria,⁽¹⁾ J. I. Amalvy,⁽²⁾ O. E. Piro,⁽³⁾ E. E. Castellano,⁽⁴⁾ and P. J. Aymonino^{(1)*}

Received September 21, 1995

The title compound, $\text{Rb}_2[\text{Fe}(\text{CN})_5\text{NO}]$, crystallizes in the space group $\text{P2}_12_12_1$, with $a = 5.687(1)$, $b = 15.956(2)$, $c = 12.645(3)$ Å, and $Z = 4$. Anions are in equivalent C_1 sites (one per asymmetric unit) and are slightly distorted octahedra (C_{4v} ideal symmetry). TGA and DTA curves and vibrational (infrared and Raman) spectra of $\text{Rb}_2[\text{Fe}(\text{CN})_5\text{NO}]$ were obtained. Results are interpreted in view of the crystal structure of the compound and the behavior of related substances.

KEY WORDS: Crystal structure; rubidium nitroprusside; IR; Raman; thermal analysis.

Introduction

The present work is part of a research program on the structural, thermal and spectroscopic properties of salts of nitroprusside and related anions.¹⁻⁸ Recently, interest in transition metal-nitrosyl complexes has been renewed due to the discovery of electronically excited metastable states of striking spectroscopic behavior in $\text{Na}_2[\text{Fe}(\text{CN})_5\text{NO}] \cdot 2\text{H}_2\text{O}$ (SNP),^{9,10} $\text{Ba}_2[\text{Fe}(\text{CN})_5\text{NO}] \cdot 3\text{H}_2\text{O}$ ¹¹ and in a whole of series of nitroprusside-containing salts (including $\text{Rb}_2\text{Npr} \cdot \text{H}_2\text{O}$, although in this and other salts only one state has been detected by DSC, a fact that we are presently studying by IR spectroscopy) as pure solids, glassy matrices

and frozen solutions.¹² These states are very long-lived at low temperatures and have potential applications in optical information storage systems. The key role of the $\text{Fe}(3d)\text{NO}$ group in the phenomenon was put into evidence by vibrational spectroscopic¹³ and neutron¹⁴ and X-ray¹⁵ diffraction methods applied to SNP. Furthermore, similar metastable states were found to occur also in other transition-metal complexes with metal(nd)NO ($n = 4, 5$) groups, including the potassium salts of $[\text{RuCl}_5\text{NO}]^{2-}$ and $[\text{Ru}(\text{NO}_2)_4(\text{OH})(\text{NO})]^{2-}$ ions^{16,17} and the (isomorphous to SNP) $\text{Na}_2[\text{M}(\text{CN})_5\text{NO}] \cdot 2\text{H}_2\text{O}$ (M : Ru,¹⁸ Os¹⁹) salts.

As a new contribution in the field of nitroprussides and in particular in the realm of the alkali metal salts, we studied rubidium nitroprusside (Rb_2Npr), which can be crystallized with no water of hydration. The interest in this salt lies precisely in its anhydrous character and one of the purposes of this work is to compare its crystal structure and spectroscopic and thermal behavior with the hydrated salt studied previously by Gentil¹ as a monohydrate and by Tosi,² also as a monohydrate and a dihydrate as well. Such a comparison could contribute to the knowledge of the role played by the water molecules in the properties of hydrated nitroprusside salts. The present study provides therefore more information about the thermal,

⁽¹⁾ Programa QUINOR, Departamento de Química, Facultad de Ciencias Exactas, Universidad Nacional de La Plata, 47 esq. 115, C.C.962, 1900 La Plata, República Argentina.

⁽²⁾ CIDEPIINT, Centro de Investigación y Desarrollo en Tecnología de Pinturas, Av. 52 entre 121 y 122, La Plata, República Argentina.

⁽³⁾ Departamento de Física, Facultad de Ciencias Exactas, Universidad Nacional de La Plata, C.C.67, 1900 La Plata, República Argentina.

⁽⁴⁾ Instituto de Física e Química de São Carlos, Universidade de São Paulo, C.P.369, 13560 São Carlos (SP), Brazil.

* To whom correspondence should be addressed.

crystallographic and spectroscopic properties of the alkaline nitroprussides series. In particular, the IR and Raman spectra constitute the reference vibrational data of $\text{Rb}_2[\text{Fe}(\text{CN})_5\text{NO}]$ in its electronic ground state to compare with the vibrational spectra of the electronically excited compound.

Garg and Goel³ reported the anhydrous salt and its main infrared stretching bands. In this work, a more detailed assignment of IR and Raman bands is performed, and thermal analysis results are also provided and discussed.

This compound is one of the two salts found to crystallize in the anhydrous state among the alkaline nitroprussides. The other one is the cesium salt⁴ which contains two inequivalent nitroprusside anions per asymmetric unit; consequently, its infrared spectrum shows duplication of several bands but no indication of correlation splitting. In the present case, all anions are equivalent and no correlation splitting has been observed. The assignment of the vibrational bands is simpler than in the cesium case. It is to be noted that the cesium salt crystallizes also as a monohydrate.²⁰

Experimental

The compound was prepared by reaction under stirring of a mixture of silver nitroprusside (obtained as a pink solid by mixing stoichiometric amounts of 0.1 M solution of sodium nitroprusside and 0.2 M of AgNO_3) and a solution of rubidium chloride (in an amount a bit less than stoichiometric) and filtering out the silver chloride formed by double decomposition. Small crystals of the rubidium salt were obtained by spontaneous evaporation of the aqueous solution at room temperature. It is to be noted that Garg and Goel³ obtained the anhydrous compound by evaporation at 50–55°C under an infrared lamp but, on the contrary, Gentil¹ obtained the monohydrate when evaporating at 50°C in a thermostat. The conditions of synthesis of the mono- and dihydrate obtained by Tosi² were not specified.

Crystal data, data collection procedure, structure determination methods, and refinement results for $\text{Rb}_2[\text{Fe}(\text{CN})_5\text{NO}]$ are summarized in Table 1.

TGA and DTA

TGA and DTA were performed with Shimadzu TGA 50 and DTA 50H units at a heating rate of 5°C/min and nitrogen flow of 50 ml/min.

Table 1. Crystal data, data collection details, and structure refinement results for $\text{Rb}_2[\text{Fe}(\text{CN})_5\text{NO}]$

Compound	$\text{Rb}_2[\text{Fe}(\text{CN})_5\text{NO}]$
Color/shape	Red/fragment
Formula weight	386.88
Space group	$P2_12_12_1$
Temp., °C	22
Cell constants ^a	
<i>a</i> , Å	5.687(1)
<i>b</i> , Å	15.956(2)
<i>c</i> , Å	12.645(3)
Cell volume, Å ³	1147.4(6)
Formula units/unit cell	4
<i>D</i> _{calc} , g·cm ⁻³	2.24
<i>μ</i> _{calc} , cm ⁻¹	95.2
Diffractometer/scan	Enraf-Nonius CAD-4/ω – 2θ
Radiation, graphite monochromator	$\text{MoK}\alpha$ ($\lambda = 0.71069$ Å)
Max. crystal dimensions, mm	0.2 × 0.15 × 0.15
Standard reflections	(4,0,0); (0,12,0); (2,2,8)
Reflections measured	1950
2θ range, deg	0 < 2θ < 60
Range of <i>h</i> , <i>k</i> , <i>l</i>	+8, +22, +17
Reflection observed [<i>F</i> _o ≤ 6σ(<i>F</i> _c)] ^b	1509
Computer programs ^c	SHELX ²¹ , SDP ²²
Structure solution ^d	SHELX ²¹
No. of parameters varied	136
Minimized function	$\sum w(F_o - F_c)^2$
Weights	$[\sigma^2(F_o + 0.0388 F_c)^{-1}]$
$R = \sum F_o - F_c / \sum F_o $	0.082
$R_w = [\sum w(F_o - F_c)^2]^{1/2} / \sum F_o $	0.082
Max. shift/σ final refinement	0.05
Largest feature final diff. map	2.1 e ⁻ Å ⁻³

^a Least-squares refinement of $[(\sin\theta)/\lambda]^2$ values for 15 reflections in the 7.90 < θ < 23.63 range.

^b Corrections: Lorentz and polarization.

^c Scattering factors for Fe²⁺ and Rb⁺, for neutral C, N, and O and neutral anomalous dispersion corrections for all atoms.

^d Structure solved by Patterson and Fourier methods and the final molecular model obtained by anisotropic full-matrix least-squares refinement.

IR and Raman spectra

The IR absorption spectra of Nujol mulls of Rb_2Npr between CsI plates were recorded at room temperature with a Perkin Elmer 580B spectrophotometer provided with an Infrared Data Station Model 3500. The spectrophotometer was routinely calibrated using water, carbon monoxide, ammonia, and sodium nitroprusside²⁵ absorption bands. The accuracy of wavenumbers reported below for sharp bands is ±1 cm⁻¹ and ±2 cm⁻¹ for broad bands.

The Raman spectrum was recorded, also at room temperature, with a Spex-Ramalog instrument provided with a Scamp microprocessor and a Spectra-Physics Kr^+ -laser tuned at 647.1 nm. The instrument was calibrated using the spectral lines of a neon lamp. Wavenumber accuracy was $\pm 1 \text{ cm}^{-1}$.

Results and discussion

Structural results

The crystal structure of the compound belongs to the orthorhombic space group $\text{P}2_12_12_1(D_2^4)$, and the anions occupy equivalent C_1 sites in the lattice but the distortion from ideal C_{4v} symmetry is slight. The asymmetric unit contains one nitroprusside anion and two rubidium cations.

Fractional coordinates and equivalent isotropic temperature parameters²⁶ for $\text{Rb}_2[\text{Fe}(\text{CN})_5\text{NO}]$ are given in Table 2. Relevant bond distances and angles within the nitroprusside ion are in Table 3. Figure 1 is a drawing of the nitroprusside anion showing the labelling of the atoms and their vibrational ellipsoids. A stereoscopic view of the crystal packing is shown in Fig. 2.

The nitroprusside ion exhibits the usual distorted octahedral configuration of ligands around iron with the equatorial Fe–C bonds slightly bent towards the axial cyanide. Fe–N, average Fe–C, N–O, and average C–N bond lengths are 1.69(1), 1.93(2), 1.19(2), and 1.18(4) Å, respectively. Fe–N–O, average Fe–C–N,

Table 3. Interatomic bond distances (Å) and angles (°) for $\text{Rb}_2[\text{Fe}(\text{CN})_5\text{NO}]$

(a) Bond distances			
Fe–N	1.69(1)	N–O	1.19(2)
Fe–C(1)	1.92(2)	C(1)–N(1)	1.18(3)
Fe–C(2)	1.92(2)	C(2)–N(2)	1.22(2)
Fe–C(3)	1.93(2)	C(3)–N(3)	1.21(2)
Fe–C(4)	1.92(2)	C(4)–N(4)	1.13(3)
Fe–C(5)	1.96(2)	C(5)–N(5)	1.15(3)
(b) Bond angles			
Fe–N–O	179(2)	C(1)–Fe–C(2)	89.5(8)
Fe–C(1)–N(1)	174(2)	C(1)–Fe–C(3)	171.3(8)
Fe–C(2)–N(2)	176(2)	C(1)–Fe–C(4)	88.3(9)
Fe–C(3)–N(3)	172(2)	C(1)–Fe–C(5)	88.0(9)
Fe–C(4)–N(4)	175(2)	C(2)–Fe–C(3)	90.2(8)
Fe–C(5)–N(5)	176(2)	C(2)–Fe–C(4)	172(1)
N–Fe–C(1)	93.9(8)	C(2)–Fe–C(5)	81.8(9)
N–Fe–C(2)	94.2(9)	C(3)–Fe–C(4)	90.8(9)
N–Fe–C(3)	94.9(8)	C(3)–Fe–C(5)	83.4(8)
N–Fe–C(4)	94.0(9)		
N–Fe–C(5)	175.6(8)		

N–Fe–C_{ax}, average N–Fe–C_{eq}, average *trans* C_{eq}–Fe–C_{eq} and average *cis* C_{eq}–Fe–C_{eq} bond angles are 179(2), 175(2), 175.6(8), 94.3(5), 172(1), and 90(1) degrees, respectively. These intramolecular distances and angles are in agreement with other determinations of nitroprusside geometry (cf., reference 27).

TGA-DTA

DTA curves show two close lying exothermic decomposition stages at 288°C and at 294°C, which

Table 2. Fractional atomic coordinates and equivalent isotropic temperature parameters²⁴ (Å²) of $\text{Rb}_2[\text{Fe}(\text{CN})_5\text{NO}]$

Atom	X/A	Y/B	Z/C	Biso
Rb(1)	0.2755(2)	0.1035(1)	−0.1173(1)	2.27(3)
Rb(2)	0.2301(2)	0.3581(1)	0.4317(1)	2.64(4)
Fe	0.0122(4)	0.3710(1)	0.7804(1)	2.84(6)
N	0.207(3)	0.375(1)	0.881(1)	3.4(4)
O	0.343(4)	0.379(1)	0.952(1)	5.4(6)
C(1)	−0.180(4)	0.288(1)	0.848(1)	3.5(5)
N(1)	−0.300(4)	0.242(2)	0.898(2)	7.3(9)
C(2)	0.176(3)	0.284(1)	0.707(2)	3.4(5)
N(2)	0.267(5)	0.227(1)	0.656(2)	6.9(9)
C(3)	0.171(4)	0.454(1)	0.695(1)	3.6(5)
N(3)	0.243(4)	0.507(1)	0.636(2)	5.5(7)
C(4)	−0.188(5)	0.456(1)	0.840(2)	4.5(6)
N(4)	−0.298(5)	0.508(1)	0.871(2)	5.6(8)
C(5)	−0.195(3)	0.362(1)	0.658(1)	3.8(5)
N(5)	−0.322(4)	0.361(1)	0.587(1)	5.0(7)

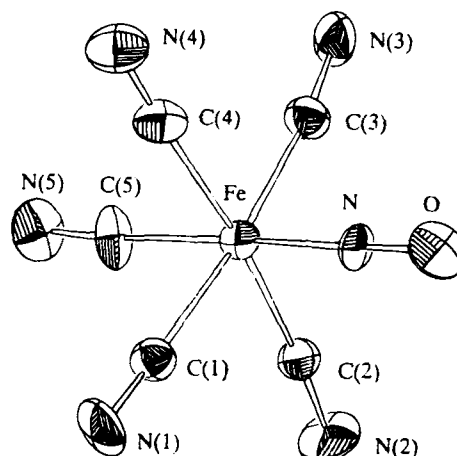


Fig. 1. ORTEP projection of the $[\text{Fe}(\text{CN})_5\text{NO}]^{2-}$ ion showing the atom numbering scheme and thermal ellipsoids at 30% probability.

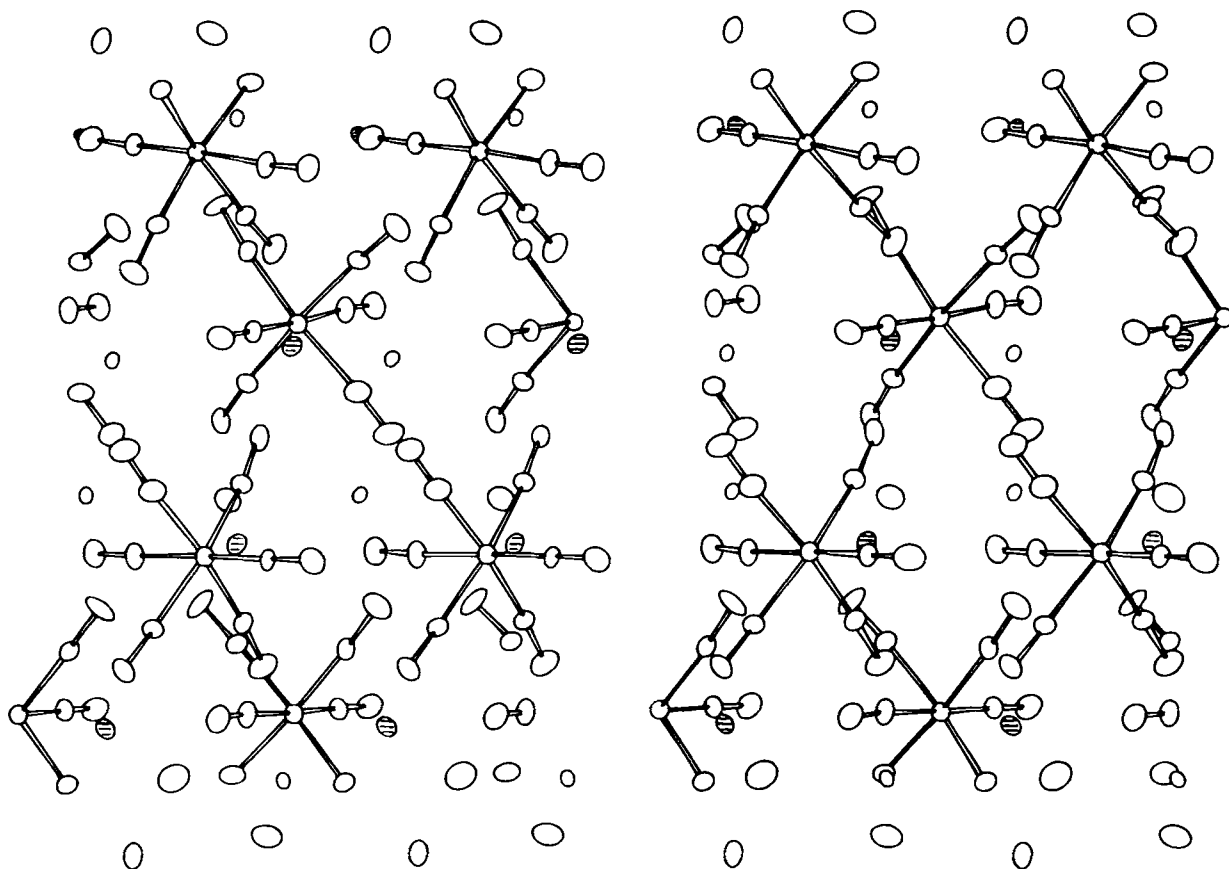
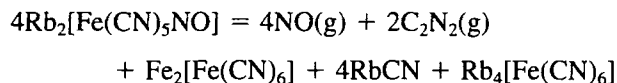


Fig. 2. ORTEP stereoscopic projection of $\text{Rb}_2[\text{Fe}(\text{CN})_5\text{NO}]$ along c showing the crystal packing. The b axis is vertical. The nitroprusside $(\text{NC})_5\text{FeNO}$ nearly rectilinear axis is approximately parallel to the horizontal (ac) plane. Hatched disks identify rubidium cations.

should correspond, respectively, to the loss of NO and C_2N_2 , as usually accepted⁵ according perhaps to the following global equation:



Total weight change observed in TGA was 14.485 mg, while the expected value from the stoichiometry of above is 14.480 mg.

IR and Raman spectra

Wavenumbers and relative intensities of the IR absorption and Raman scattering bands due to the anion, as well as their tentative assignments, are reported in Table 4. Wavenumbers now reported do not differ significantly from values reported for the hydrated salts.²

As there is only one crystallographic type of anion in Rb_2Npr , which is only slightly distorted from C_{4v} symmetry, and because it seems that the vibrational interaction in the unit cell is negligible, as there are no band splittings, the vibrational behavior will be discussed on the C_{4v} basis. In what follows, wavenumbers refer to the IR spectrum unless otherwise stated (R for Raman).

CN stretching bands

Three bands are observed at 2153(vw), 2148(vw), and 2136(vs) cm^{-1} , which can be assigned to the CN stretching vibrations. In the Raman spectrum features are observed at 2154(m), 2149(s), 2144(m) and 2138(w) cm^{-1} . Bands due to isotopically most abundant $^{12}\text{C}^{14}\text{N}$ groups can be assigned on the basis of the relative intensities and by comparison with other nitroprusside salts.^{4,8,28-32}

Table 4. Observed IR and Raman bands and assignments for the anion in $\text{Rb}_2[\text{Fe}(\text{CN})_5\text{NO}]^a$

Symmetry species under C_{4v}	Raman (r.t.)	IR (r.t.)	Assignment
		3842(vw)	$2\nu\text{NO}$
A_1	2154(m)	2153(vw)	νCN_{ax}
A_1	2149(s)	2148(vw)	νCN
B_1	2144(m)		νCN
E	2138(w)	2136(vs)	νCN
		2110(sh)	$\nu^{12}\text{C}^{15}\text{N}$
		2093(vw)	$\nu^{13}\text{C}^{14}\text{N}$
A_1		1931(vs)	νNO
		1893(sh)	$\nu^{14}\text{N}^{18}\text{O}$
E		658(m)	δFeNO
A_1	654(s)	653(sh)	νFeN
		496(vw)	$\delta\text{FeCN}_{\text{ax}}$
	458(m)	452(vw)	$\nu\text{FeC}_{\text{ax}}$
		428(vw)	νFeC
		418(w)	νFeC
	411(w)	410(w)	νFeC
	401(w)	403(s)	νFeC
	392(m)	390(sh)	νFeC
		319(w)	δFeCN
		303(sh)	?
	168(s)		l.m.
	147(s)		δCFeN
	136(s)		l.m.
	124(s)		δCFeN
	105(s)		$\delta\text{CFeC}_{\text{ax}}$
	91(vs)		$\delta\text{CFeC} + \delta\text{CFeN}$

^a data in cm^{-1} ; r.t.: room temperature; vs: very strong; s: strong; m: medium; w: weak; vw: very weak; sh: shoulder; l.m.: lattice mode.

Note: C and C-bonded N atoms are equatorial unless explicitly mentioned as axial.

Bands at 2153(vw) and 2154(m) (R) cm^{-1} are assigned to the A_1 (axial) mode. The features at 2148(vw) and 2149(s) cm^{-1} (R) should be assigned to the A_1 (equatorial) mode (activated in IR by the departure from planarity of the equatorial CN groups). The band at 2144(m) cm^{-1} (R) should be due to the B_1 (equatorial) mode and those at 2136(vs) and 2138(vw) cm^{-1} (R), to the E (equatorial) mode.

The very weak features observed at 2110 (sh) and 2093 cm^{-1} are due to isolated $^{12}\text{C}^{15}\text{N}$ and $^{13}\text{C}^{14}\text{N}$ equatorial groups, respectively. The assignment of the latter band to $^{12}\text{C}^{15}\text{N}$ is precluded by the fact that, in that case, a $^{13}\text{C}^{14}\text{N}$ peak three times more intense would be expected at a wavenumber 11–17 cm^{-1} lower.³⁰ Features hereby discussed seem to fulfil these relationships.

NO and FeNO vibrational bands

The very strong band at 1931 cm^{-1} is assigned to the stretching of the NO group. The shoulder at 1893 cm^{-1} should be due to isotopic NO groups. In sodium nitroprusside dihydrate,²⁹ the relative wavenumbers of the stretching bands of the $^{15}\text{N}^{16}\text{O}$ (0.38% natural abundance) and $^{14}\text{N}^{18}\text{O}$ (0.20% abundance) isotopic species referred to $\nu^{14}\text{N}^{16}\text{O}$ are in the ratios: 1:0.984:0.981, respectively. Therefore, in the present case, the expected values for these species should be 1900 and 1894 cm^{-1} . Consequently, the observed shoulder at 1893 cm^{-1} is assigned to $^{14}\text{N}^{18}\text{O}$ groups. The other band is surely hidden by the main band.

The very weak band at 3842 cm^{-1} is due to the first overtone of the νNO band. The difference with $2\nu\text{NO}$, due to anharmonicity, is 20 cm^{-1} , while in $\text{Na}_2\text{Npr} \cdot 2\text{H}_2\text{O}$, is 17.6 cm^{-1} , in which case a value of 10.15 cm^{-1} has been determined for the anharmonicity coefficient, $\bar{\omega}_e x_e$. It is to be noted that in the sodium nitroprusside spectrum, this band appears at 3872 cm^{-1} and the fundamental at 1940 cm^{-1} .²⁸

As usual, the feature at 658 (m) cm^{-1} is assigned to the FeNO deformation and those at 653(sh) and 654(s) cm^{-1} (R), to the FeN stretching.

FeC stretchings and FeCN deformations

The assignment of bands supposedly due to these modes (Table 4) was made from assignments in reference 28.

CFeC and CFeN deformations

These bands appear below 180 cm^{-1} (cf. 28,30) and were observed only in the Raman spectrum. Assignments also follow those in reference 28.

Conclusions

The crystal structure of the present compound, in comparison with the known structures of hydrated nitroprussides,^{27,33,34} does not show any particular characteristic to be traced to the absence of water molecules, suggesting that water does not play a pre-dominant ordering role in the hydrated compounds. The similitude of wavenumbers of vibrational bands of

the anion in the anhydrous compound and the hydrates points to a negligible water–anion interaction.

It is to be noted that no band splitting has been observed either in the IR or the Raman spectrum of Rb_2Npr , in accordance with the X-ray determination, which shows the existence of only one type of nitroprusside ion in the lattice and unfavorable mutual orientations of the anions and distances between them to give place to a noticeable vibrational coupling of the strongly polar NO groups in the unit cell as it occurs in other nitroprusside salts.³⁵ Interestingly enough, the present work is the second concerning an anhydrous alkaline nitroprusside but in this case, the crystal and vibrational structures are simpler than in the previously reported (cesium) salt.⁴

Acknowledgments

We thank CONICET through Programa QUINOR, PID-BID #252-0108/91 and PROFIMO and CICPBA, República Argentina, and FINEP and FAPESP, Brasil, for financial support.

References

- Gentil, L.A. *Doctoral Thesis*, Facultad de Ciencias Exactas, Universidad Nacional de La Plata, R. Argentina, 1973.
- Tosi, L. *Compt. Rend.* **1973**, 277C, 335.
- Garg, A.N.; Goel, P.S. *Inorg. Chem.* **1971**, 109, 1345.
- Vergara, M.M.; Varetti, E.L.; Rigotti, G.; Navaza A. *Phys. Chem. Solids* **1989**, 50, 951.
- Zuriaga, M.J.; Monti, G.A.; Martin, C.A.; Güida, J.A.; Piro, O.E.; Aymonino, P.J. *J. Thermal Analysis* **1991**, 37, 1523.
- Güida, J.A.; Piro, O.E.; Aymonino, P.J.; Sala, O. *J. Raman Spectrosc.* **1992**, 23, 131.
- Chacón Villalba, M.E.; Varetti, E.L.; Aymonino, P.J. *Vibrational Spectrosc.* **1992**, 4, 109.
- Soria D.B.; Aymonino, P.J. *Spectrochim. Acta* **1995**, 51A, 677.
- Hauser, U.; Oestreich, V.; Rohrweck, H.D. *Z. Phys.* **1977**, A280, 17; **1997**, A280, 125; **1978**, A284, 9.
- Güida, J.A.; Piro, O.E.; Aymonino, P.J. *Solid State Commun.* **1986**, 57, 175.
- Güida, J.A.; Piro, O.E.; Aymonino, P.J. *Solid State Commun.* **1988**, 66, 1007.
- Zöllner, H.; Krasser, W.; Woike, Th.; Haussühl, S. *Chem. Phys. Letters* **1989**, 161, 497.
- Güida, J.A.; Aymonino, P.J.; Piro, O.E.; Castellano, E.E. *Spectrochim. Acta* **1993**, 49A, 535.
- Rüdlinger, M.; Schefer, M.J.; Chevrier, G.; Furer, N.; Güdel, H.U.; Haussühl, S.; Heger, G.; Schweiss, P.; Vogt, T.; Woike, Th.; Zöllner, H. *Z. Phys.* **1991**, B83, 125; Rüdlinger, M.; Schefer, J.; Vogt, T.; Woike, Th.; Haussühl, S.; Zöllner, H. *Physica* **1992**, B180–181, 293.
- Pressprich, M.R.; White, M.A.; Vekhter, Y.; Coppens, P. *J. Am. Chem. Soc.* **1994**, 116, 5233.
- Woike, Th.; Zöllner, H.; Krasser, W.; Haussühl, S. *Solid State Commun.* **1990**, 73, 149.
- Woike, Th.; Haussühl, S. *Solid State Commun.* **1993**, 86, 333.
- Piro, O.E.; Güida, J.A.; Schaiquevich, P.S.; Aymonino, P.J. *80th National Physics Meeting*, October 2–6, 1995, Bariloche, R. Argentina, to be published elsewhere.
- Güida, J.A.; Piro, O.E.; Aymonino, P.J. *Inorg. Chem.* **1995**, 34, 4113.
- Vergara, M.M.; Varetti, E.L. *J. Phys. Chem. Solids* **1987**, 48, 13.
- Cromer, D.T.; Waber, J.T. in *International Tables for X-ray Crystallography*; Kynoch Press: Birmingham, England, 1974; Vol. IV, p. 71. Cromer, D.T.; Ibers, J.A. *ibid.*; p. 149.
- Sheldrick, G.M. *SHELX, a Program for Crystal Structure Determination*; University of Cambridge, Cambridge, England, 1976.
- Frenz, B.A. *Enraf-Nonius Structure Determination Package*; Enraf-Nonius: Delft, The Netherlands, 1983.
- Johnson, C.K. *ORTEP. Report ORNL-3794*, Oak Ridge, TN, 1965.
- Della Védova, C.O.; Lesk, J.H.; Varetti, E.L.; Aymonino, P.J.; Piro, O.E.; Rivero, B.E.; Castellano, E.E. *J. Mol. Struct.* **1981**, 70, 241.
- Hamilton, W.C. *Acta Crystallogr.* **1959**, 12, 609.
- Amalvy, J.I.; Varetti, E.L.; Aymonino, P.J.; Castellano, E.E.; Piro, O.E.; Punte, G. *J. Cryst. Spectrosc. Res.* **1986**, 16, 537.
- Chacón Villalba, M.E. *Doctoral Thesis*, Facultad de Ciencias Exactas, UNLP, Argentina, 1995, to be published elsewhere.
- Holzbecher, M.; Knop, O.; Falk, M. *Can. J. Chem.* **1971**, 49, 1413.
- Bates, J.B.; Khanna, R.K. *Inorg. Chem.* **1970**, 491, 1376.
- Swanson, B.I.; Jones, L.H. *Inorg. Chem.* **1974**, 13, 313.
- Paliani, G.; Poletti, A.; Santucci, A. *J. Mol. Struct.* **1971**, 8, 63.
- Alvarez, A.G.; Aymonino, P.J.; Baran, E.J.; Gentil, L.A.; Lanfrancini, L.H.; Varetti, E.L. *J. Inorg. Nucl. Chem.* **1976**, 38, 221.
- Navaza, A.; Schweiss, P.; Alzari, M.; Chevrier, G.; Heger, G.; Güida, J.A. *Solid State Chem.* **1990**, 89, 23.
- González, S.R.; Piro, O.E.; Aymonino, P.J. *J. Chem. Phys.* **1984**, 81, 625.

SUPPLEMENTARY MATERIAL. Crystallographic data (excluding structure factors) for the structure reported in this paper has been deposited with the Cambridge Crystallographic Data Centre as supplementary publication no. CCDC-1003/5023. Copies of available material can be obtained, free of charge, on application to the Director, CCDC, 12 Union Road, Cambridge CB2 1EZ, UK, (fax: +44-(0)1223-336033 or e-mail: teched@chemcrs.cam.ac.uk).